Nuclear Instruments and Methods in Physics Research A250 (1986) 183–191
North-Holland, Amsterdam

FEASIBILITY OF HIGH GAIN X-RAY FREE ELECTRON LASERS

A. GOVER [1], E. JERBY [1], J.E. LaSALA [2] and D.A.G. DEACON [3]

[1] *Faculty of Engineering, Tel-Aviv University, Ramat-Aviv 69978, Israel*
[2] *High Energy Physics Laboratory Stanford University, Stanford, CA 94305, USA*
[3] *Deacon Research, 900 Welch Road Suite 203, Palo Alto, CA 94304, USA*

We investigate the feasibility of a tunable VUV/soft X-ray FEL operating in a dedicated storage ring. Because of poor mirror reflectivity available at these wavelengths, the FEL must operate in the intermediate high gain regime (gain = 3–5). In order to obtain this high gain, a long interaction length (27 m), a high current (270 A) and strong magnetic fields ($\bar{a}_w > 1$) are necessary. Consequently some velocity spread effects and possibly even some space charge effects must be considered. We use a one-dimensional, comprehensive small signal gain analytical model to conduct a parametric study of the FEL operating parameters and their scaling laws. The results of the analytic model are compared with results obtained with the 2-D FEL simulation code FRED, and the effect of optical guiding on the gain is estimated using an enhanced filling factor based on the observed guided mode size. We conclude that oscillation below 300 Å is feasible with existing mirror technology.

1. Introduction

Since the first demonstration of a free electron laser (FEL) amplifier [1] and oscillator [2], at 10.6 and 3.4 μm wavelengths, respectively, much research effort has been directed towards short wavelength operation of FELs. Whereas the first experiments were carried out with a superconducting linac, shorter visible wavelength lasing (6400 Å) was obtained recently with an optical klystron operating in a storage ring [3]. Visible wavelength radiation at the third harmonic (and possibly lasing) was also measured in another recent experiment at 5300 Å, using again a superconducting linac [4].

A number of proposals have been made for operating FELs in the short wavelength UV and X-ray regime [5–7]. There is, of course, considerable interest in the development of presently nonexistent high-power bright coherent sources in the X-ray regime. Considering only scientific aspects, such development will bear a significant impact on the field of microbiology, biochemistry, material sciences, radiology, medical diagnostics and treatment. Recent technological progress makes it now possible for us to predict, on the basis of reliable basic theory, the feasibility of laser operation in the soft X-ray wavelength regime. We use in this study the electron beam parameters expected to be realizable with present storage ring accelerator technology [8]. A study carried out recently at Los Alamos National Laboratory also suggested the feasibility of VUV FELs operating at wavelengths down to 500 Å [9] utilizing a pulsed rf linac. Our study, based on the design parameters of a FEL dedicated storage ring [10], suggests the feasibility of X-ray FELs operating at wavelengths down to 300 Å.

One of the main obstacles thus far in realizing X-ray oscillators is the present poor state-of-the-art of laser mirrors at wavelengths below 100 Å [11]. The low mirror reflectivity presently available, or feasible in the near future, directs us to consider FEL operation in the high gain regime. If we consider $R = 60\%$ as an attainable mirror reflectivity value, and would like to have, say, $T = 10\%$ transmission through one end, then a minimum single-pass gain of $G \equiv P_{out}/P_{in} = 3.2$ is necessary in order to reach the oscillation threshold. Basic FEL small signal gain theory [12] indicates that long interaction length and high peak current are necessary to obtain such a high gain. However, in most accelerators, high peak current requirements lead to pour beam quality parameters (energy spread and emittance) [13]. This may cause the laser to operate in the warm beam regime, where gain is substantially reduced relative to a cold beam [14]. The longer interaction length, the better the beam quality parameters should be in order to maintain operation in the cold beam regime. This results in a trade-off between the long interaction length

requirement and the high current requirement. This contradictory requirement dilemma is somewhat relieved if operation in the high gain regime is feasible because then the beam quality acceptance parameters of the FEL are relaxed [14].

The discussion above gives the rationale for choosing a storage ring for soft X-ray FEL operation. In a storage ring, high instantaneous current (hundreds of amperes) is quite readily available, while the beam quality parameters (emittance, energy spread) stay very small. This suggests that in order to study the limits of X-ray wavelength operation of FELs, a comprehensive small signal analytical model should be used, including high gain, exact axial velocity spread, and space-charge (longitudinal plasma waves) effects [15]. Using the basic design parameters of the Stanford FEL dedicated storage ring, we calculate the gain at the first and third harmonics of various wiggler schemes. The results show considerable gain at 300 Å wavelength.

2. The theoretical model

The theoretical model that is used in this paper is based on the solution of maxwell's equations, simultaneously with the linearized Vlasov equation with characteristic lines adequate to the electron trajectories in a strong planar Wiggler [15]. This results in a gain dispersion relation at the $2n+1$ harmonic wavelength, as follows:

$$\left.\frac{\bar{E}(s)}{E(0)}\right|_{2n+1} = \frac{\left[1+J_n^2(\ )\chi_{2n+1}\right]\left[1+J_{n+1}^2(\ )\chi_{2n+1}\right]}{(s-\mathrm{i}k_{z0})\left[1+J_n^2(\ )\chi_{2n+1}\right]\left[1+J_{n+1}^2(\ )\chi_{2n+1}\right]} \times \frac{1}{-\mathrm{i}\kappa_{2n+1}\left[J_n(\ )-J_{n+1}(\ )\right]^2\left[1+J_n(\ )J_{n+1}(\ )\chi_{2n+1}\right]\chi_{2n+1}}. \tag{1}$$

The argument of all Bessel functions is:

$$\alpha_{2n+1} = \frac{1}{2}\frac{\bar{a}_w^2}{1+\bar{a}_w^2}(2n+1), \tag{2}$$

where

$$\bar{a}_w = \frac{eB_w}{\sqrt{2}\,mck_w} \tag{3}$$

is the normalized rms vector potential of the static planar wiggler field

$$\boldsymbol{B}_w = \hat{x}B_w \sin k_w z.$$

The longitudinal susceptibility of the electron beam $\chi(s)$ is defined by:

$$\chi(s) = -\frac{\mathrm{i}e^2}{\omega}\int \frac{\partial f(\bar{P}_z)}{\partial P_z}\frac{\mathrm{d}P_z}{s-\mathrm{i}\omega/\bar{V}_z}, \tag{4a}$$

and

$$\chi_{2n+1} \equiv \chi\left(s+\mathrm{i}(2n+1)k_w\right)/\epsilon_0. \tag{4b}$$

The "exact" axial momentum distribution can be evaluated for a storage ring FEL, assuming that the electron total energy, $E=\gamma_0 mc^2$, and the electrons initial angle at the wiggler entrance, ϕ, are Gaussian distributed independent random variables [8] with standard deviations of $\Delta E/\sqrt{2}$ and $\Delta\phi/\sqrt{2}$, respectively. This results in the normalized distribution function [15,16]:

$$f(x) = R\,\exp\left[R(R+2x)\right]\,\mathrm{erfc}(R+x), \tag{5}$$

where we assume the optimal beam radius to be:

$$r_{b0} = \frac{\Delta\phi}{k_\beta} \tag{6}$$

and use the definitions:

$$x \equiv \frac{\bar{V}_z - \bar{V}_{0z}}{\bar{V}_{0z}\delta\gamma}, \tag{7a}$$

$$\delta\gamma \equiv \frac{\Delta\gamma/\gamma_0}{\gamma_{0z}^2}, \tag{7b}$$

$$R \equiv \frac{\delta\gamma}{\Delta\phi^2}, \tag{7c}$$

$$\gamma_{0z} \equiv \frac{\gamma_0}{\left(1+\bar{a}_w^2\right)^{1/2}}, \tag{7d}$$

and

$$k_\beta = \frac{k_w \bar{a}_w}{\gamma_0} \tag{7e}$$

is the betatron oscillation wavenumber. The complementary error function $\mathrm{erfc}(x)$ is defined by:

$$\mathrm{erfc}(x) \equiv \frac{2}{\sqrt{\pi}} \int_x^\infty \mathrm{e}^{-t^2}\,\mathrm{d}t. \tag{7f}$$

The longitudinal susceptibility of the electron beam, using the "exact" distribution of eq. (5), becomes [15]:

$$\chi(s) = \frac{\epsilon\theta_p^2}{s^2\delta\gamma} 2R \int_0^\infty \mathrm{e}^{-2Ry} Z'(\xi+y)\,\mathrm{d}y, \tag{8}$$

where θ_p, the space-charge parameter, is defined by

$$\theta_p = \left[\frac{eI_0}{\pi mc^2 \epsilon r_{b0}^2 \gamma_{0z}^2 \gamma_0}\right]^{1/2}. \tag{9}$$

$Z(\xi)$ is the well known plasma dispersion function (the complex error function) and its argument ξ is given by:

$$\xi = \frac{\mathrm{i}\omega/s - \bar{V}_{0z}}{\bar{V}_{0z}\delta\gamma}. \tag{10}$$

The contribution of the energy spread to the total detuning spread of the FEL can be estimated by the detuning spread parameter due to energy spread:

$$\bar{\theta}_{th}\left(\frac{\Delta E}{E}\right) = 4\pi(2n+1)N_w\frac{\Delta E}{E}. \tag{11}$$

The parameter R gives the ratio between the contributions of the energy spread and the emittance to the detuning spread.

The coupling parameter κ in eq. (1) is expressed in this case in the form:

$$\kappa_{2n+1} = \pi N_w \frac{\bar{a}_w^2}{1+\bar{a}_w^2}(2n+1)\mathrm{FF}, \tag{12}$$

where we used the synchronism condition of the $2n+1$ harmonic:

$$\lambda_{2n+1} = \frac{\lambda_w}{2\gamma_{0z}^2(2n+1)}. \tag{13}$$

IV. HIGH GAIN FELS

The filling factor FF in eq. (12) is given for small free space diffraction of the e.m. radiation beam by:

$$FF_{fs} = \frac{1}{1 + \frac{\omega_0^2}{2r_{b0}^2}}, \tag{14}$$

where ω_0, the Gaussian mode waist size, is given in the case where the interaction length L is twice the Rayleigh length Z_R and the focusing is optimal, by:

$$\omega_0 = \sqrt{\frac{\lambda_{2n+1} L}{2\pi}}. \tag{15}$$

The assumption of free space diffraction may lead to underestimation of the gain in the high gain regime where the effect of optical guiding by the electron beam [17,18] may confine the e.m. beam to a smaller waist size than in free space. This effect leads to a higher effective filling factor, and therefore to a higher coupling parameter value and higher gain. For cases in which optical guiding occurs, we approximate the effect by using the filling factor of eq. (14) with ω_0 replaced by the radius of the focused e.m. radiation beam. This enhanced filling factor is denoting by FF_{og} (optically guided).

In the next section, we describe the results of the gain calculation in various cases. This was done in each case by combining the results of two computer codes. The FRED 2-D simulation code [19] was operated to find the waist size of the e.m. radiation beam in each case. In the cases considered here the amplified mode exhibited guiding once exponential power growth began. The resulting guided mode size was used to estimate an enhanced filling factor and was fed to the extended WARM program in order to solve the gain dispersion relation (1), including space-charge and "exact" electron distribution (eq. (5)) effects.

3. The numerical results

Using the model described in the previous section we calculated the gain at the first and third harmonics for various FEL schemes considered for implementation in the Stanford FEL dedicated storage ring. The aim of this investigation was to check the feasibility of building up to oscillation at 300 Å wavelength, which requires a small signal gain of at least 3.2 per pass.

The basic electron beam parameters of the Stanford storage ring are [10]:

$$\gamma_0 = 2000, \quad I_0 = 270\ \text{A}, \quad \epsilon_x = \epsilon_y = \pi \times 1.7 \times 10^{-8}\ (\text{m rad}), \quad \frac{\Delta E}{E} = 8.2 \times 10^{-4}.$$

The maximum wiggler length L is 27 m and the minimum gap between the poles is 30 mm. Three different wiggler schemes with periods of 11.4, 8.3 and 6.4 cm, and magnetic field densities (on the axis) of 7.2, 5.25 and 3.8 kG respectively, have been considered. The resulting FEL parameters of the various cases are listed in table 1.

In case 1 ($\lambda_w = 0.114$ m), the fundamental radiation wavelength is relatively long (4300 Å) and free space diffraction leads to a small filling factors: $FF_{fs} = 0.11$. The resonance detuning curves in fig. 1 for the first and third harmonic are based on this free space filling factor. The electron beam in case 1 may be considered cold as the fundamental wavelength is relatively long ($\bar{\theta}_{th} = 2.44$ and $R = 2.4$), but is quite warm at the third harmonic ($\bar{\theta}_{th} = 7.3$). Therefore, the third harmonic gain is further reduced relative to the fundamental harmonic gain. Our estimation for the gain at the fundamental is improved by using the FRED 2-D code to determine the guided mode size, which is then used to estimate an improved filling factor. In this case $FF_{og} = 0.38$, which provides much higher gain. The detuning curve resulting from the use of the improved filling factor is presented in fig. 2, together with the gain curve generated by FRED and the free space curve of fig. 1 (the fundamental) for comparison.

Table 1
The resulting FEL parameters for the three cases (MKS units)

Parameter	Case 1		Case 2		Case 3	
	1st har.	3rd har.	1st har.	3rd har.	1st har.	3rd har.
λ_w	0.114	0.114	0.083	0.83	0.064	0.064
N_w	237	237	325	325	422	422
$\bar{a}_w$	5.4	5.4	2.87	2.87	1.6	1.6
k_β	0.15	0.15	0.11	0.11	0.08	0.08
r_{b0}	3.4×10^{-4}	3.4×10^{-4}	4.0×10^{-4}	4.0×10^{-4}	4.6×10^{-4}	4.6×10^{-4}
γ_{0z}	364	364	658	658	1060	1060
λ_{2n+1}	4.3×10^{-7}	1.4×10^{-7}	9.6×10^{-8}	3.3×10^{-8}	2.85×10^{-8}	9.5×10^{-9}
ω_0 (fs)	1.4×10^{-3}	7.8×10^{-4}	6.4×10^{-4}	3.7×10^{-4}	3.5×10^{-4}	2.0×10^{-4}
ω_g (guided)	6.0×10^{-4}	–	4.6×10^{-4}	–	3.4×10^{-4}	–
FF_{fs}	0.11	0.27	0.43	0.7	0.776	0.96
FF_{og}	0.38	–	0.59	–	0.785	–
$\bar{\theta}_{th}(\Delta E/E)$	2.44	7.34	3.36	10.1	4.35	13.0
R	2.4	2.4	1.03	1.03	0.54	0.54
α_{2n+1}	0.48	1.45	0.45	1.34	0.36	1.08
$[JJ]^2_{2n+1}$	0.501	0.11	0.54	0.11	0.62	0.11
κ_{fs}	79.0	583.0	391.0	1912.0	744.0	2746.0
κ_{og}	278.0	–	536.0	–	753.0	–
θ_p	1.23	1.23	0.58	0.58	0.31	0.31
G_{max} (fs)	54.0	16	39.9	3.5	5.5	1.2
G_{max} (og)	1881	–	83.4	–	8.0	–
G_{max} (FRED)	682	–	72.2	–	7.9	–

We note at once in fig. 2 that the 1-D gain curve c resulting from use of the enhanced filling factor is nearly three times higher than that generated by the FRED code, curve b. We believe this discrepancy is due to the effects of diffraction. The interaction region is almost ten times longer than the input Rayleigh length for the guided mode solution realized with FRED, and the electron beam is small ($r_{b0} = 340$ μm) compared to the radius of the guided mode ($\omega_g = 600$ μm). Using as a model the work of Moore [17], we expect these scale differences to result in a guided mode gain length smaller than that of the one-dimensional theory using an enhanced filling factor. In Moore's notation, we have $\hat{a} \cong 1.0$ in this case, which is

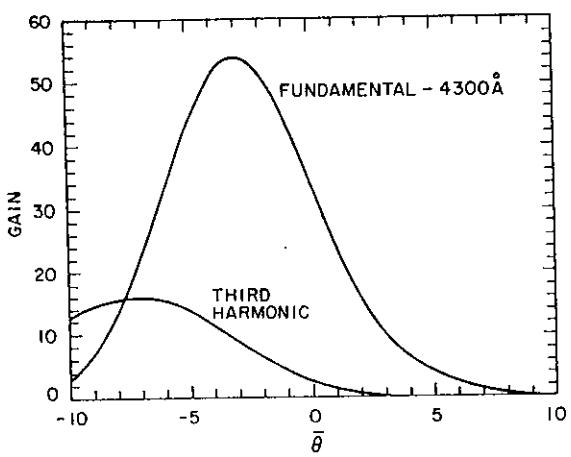

Fig. 1. Calculated single pass gain (P_{out}/P_{in}) as a function of resonance detuning parameter $\bar{\theta} = (\omega/v_{0z} - k_w - \omega/c)L$ for the fundamental (4300 Å) and third harmonic (1433 Å) in the Stanford Storage Ring FEL, obtained from solutions of the one-dimensional gain dispersion relation eq. (1) for free space input parameters of table 1, case 1.

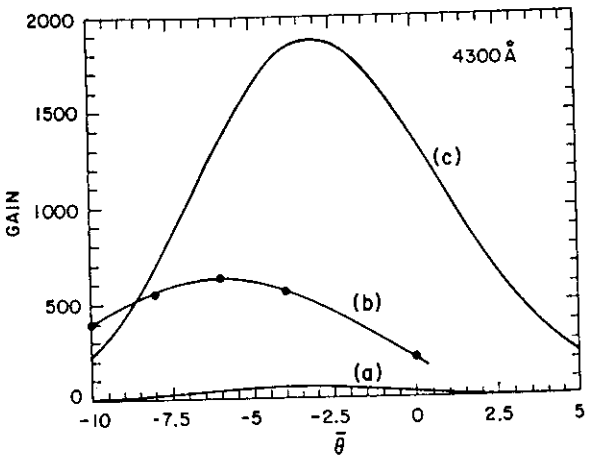

Fig. 2. Gain detuning curves for the fundamental (4300 Å) of case 1: (a) same as fundamental curve in fig. 1, (b) result of FRED 2-D [19] code simulation in which input e.m. mode focusing is optimized for maximum peak gain, (c) same as (a) but using enhanced filling factor FF_{og} estimated from guided mode size determined by FRED. Relevant parameters are given in table 1, case 1.

an indicator that 3-D effects (diffraction) are important. Here $\hat{a}$ is a "scaled" electron beam radius, whose value varies inversely with the important of diffraction. The discrepancy in gain lengths, although expected to be modest (perhaps 10–20%), would result in a large difference in overall gain after 27 m of exponential growth, as is observed to be the case.

In case 2 ($\lambda_w = 8.4$ cm), the fundamental harmonic (960 Å) is less diffracted in free space than in case 1 (4300 Å); thus the effect of optical guiding on the gain is more moderate. The contribution of the emittance to the axial velocity spread is not negligible ($R = 1.03$), and the "exact" axial velocity distribution function must be called for. Even though the gain at the third harmonic (320 Å) is considerably reduced due to the axial velocity spread, its peak value $G_{max} = 3.5$ is high enough to build up and maintain oscillation at this wavelength. Fig. 3 displays the resonance detuning curves for the fundamental and third harmonic, generated with the free space filling factor. In fig. 4 we plot for this case the detuning curves analogous to those of fig. 3. Note that the corrected filling factor curve c and the FRED curve b are in better agreement than in case 1. This is to be expected, since 3-D effects are somewhat less important in this case, although not negligible (Moore's parameter $\hat{a} \cong 3.0$).

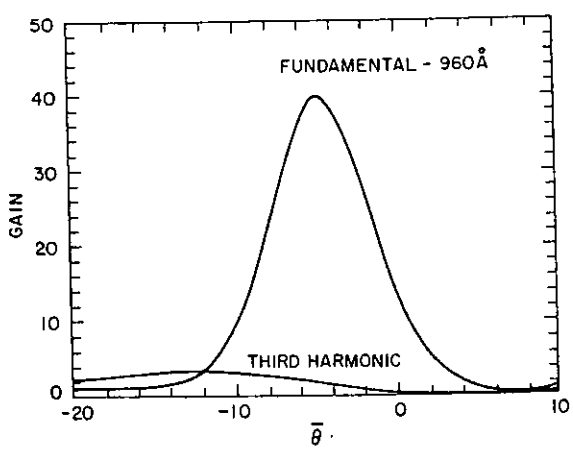

Fig. 3. Gain as a function of resonance detuning parameter for the fundamental (960 Å) and third harmonic (320 Å) obtained from solutions of the one-dimensional gain dispersion relation eq. (1) for free space input parameters of table 1, case 2.

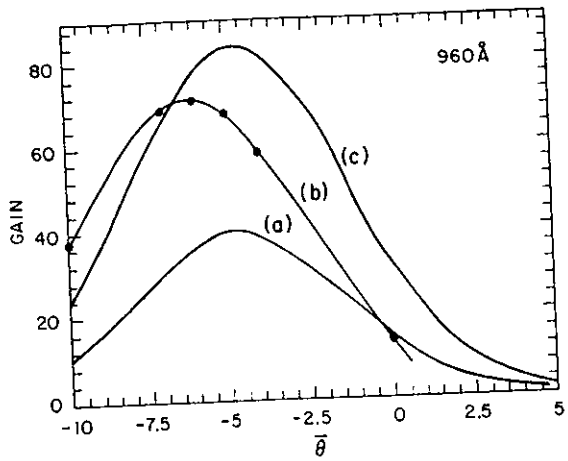

Fig. 4. Gain detuning curves for the fundamental (960 Å) of case 2: (a) same as fundamental curve in fig. 3, (b) result of FRED 2-D code simulation in which input e.m. mode focusing is optimized for maximum peak gain, (c) same as (a) but using enhanced filling factor FF_{og} estimated from guided mode size determined by FRED. Relevant parameters are given in table 1, case 2.

Although we could utilize the third harmonic of case 2 to achieve short wavelength oscillation, we obtain higher gain $G_{max} = 5.5$ at an even shorter wavelength (285 Å) at the fundamental harmonic in case 3 ($\lambda_w = 6.4$ cm). Fig. 5 exhibits the free space detuning curves for the fundamental and third harmonic for this case. The third harmonic, at a wavelength of 95 Å, interacts with a very warm electron beam ($\bar{\theta}_{th} = 13$, $R = 0.54$), but still produces measurable gain, $G_{max} = 1.23$. However, it is not sufficient to build up oscillation with the existing mirrors at this wavelength. The contribution of the emittance to the axial velocity spread is dominant in case 3 ($R = 0.54$), resulting in a skewed asymmetric distribution function. This is shown in fig. 7, where the normalized distribution function (5) is shown for $R = 2.5$, 1. and 0.5, with respect to cases 1, 2, and 3.

In performing our comparison with FRED in case 3, we expect diffraction to play a minor role, since $\hat{a} \cong 7.0$. The guided mode size given by FRED for this case is very nearly equal to that of the free space waist (table 1), so that our "enhanced" filling factor FF_{og} differs little from the free space value. We have plotted in fig. 6 the common resonance detuning curve (a) for these nearly equal filling factors. According to Moore [17], for large values of $\hat{a}$ we should expect the gain predicted by FRED to approach that

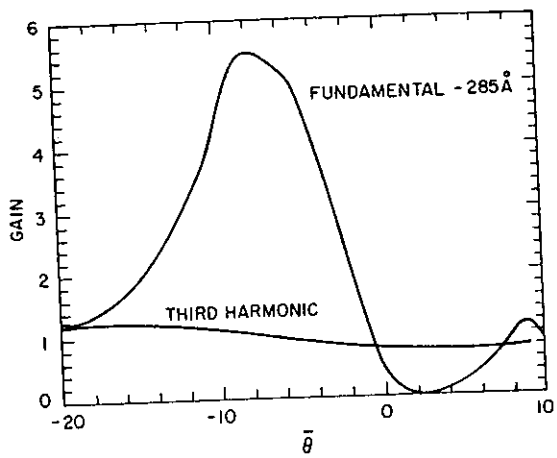

Fig. 5. Gain as a function of resonance detuning parameter for the fundamental (285 Å) and third harmonic (95 Å) obtained from solutions of the one-dimensional gain dispersion relation eq. (1) for free space input parameters of table 1, case 3.

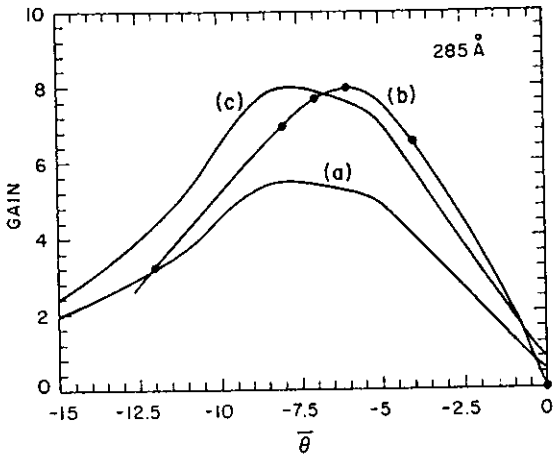

Fig. 6. Gain detuning curves for the fundamental (285 Å) of case 3: (a) same as fundamental curve in fig. 5, (b) result of FRED 2-D code simulation in which input e.m. mode focusing is optimized for maximum peak gain, (c) same as (a) but using maximum filling factor FF = 1.0. Relevant parameters are given in table 1, case 3.

calculated from 1-D theory using a filling factor of 1. To check this limit we have calculated the gain with our one-dimensional model using a filling factor of 1.0, the results of which are shown as curve c of fig. 6. Curve b of this figure is the FRED result, which compares favorably with the filling factor of 1 of the 1-D curve, both of which exceed the free space 1-D gain curve.

We note in figs. 2, 4 and 6 differences in resonance detuning behavior. The FRED curves peak at nearly the same value of detuning parameter (-6.0), while the 1-D curves show a systematic shift with wavelength. Since diffraction alters the phase of the propagating radiation as a function of radius, even when optical guiding occurs (see, for example, refs. [20,21]), we expect the detuning behavior to be difficult to obtain correctly with a 1-D theory. We do not attach much significance to the small discrepancies in detuning observed between the 1-D model and FRED.

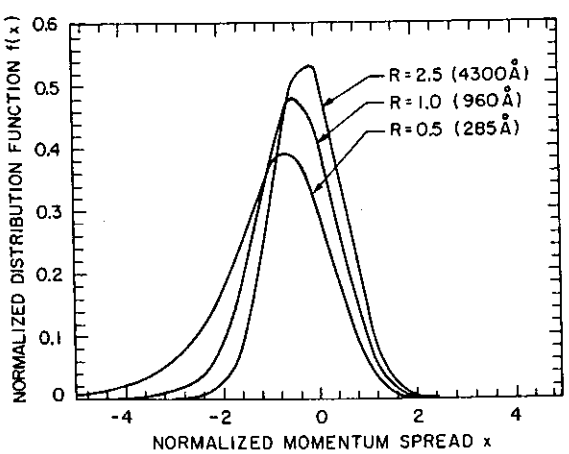

Fig. 7. Normalized "exact" axial momentum distribution function $f(x)$ of eq. (5) as a function of normalized axial momentum spread x defined in eq. (7a) for three values of R, the ratio of energy spread to emittance contributions to total momentum spread, corresponding to the three cases depicted in figs. 1–6.

4. Conclusion

The goal of obtaining laser oscillation at 300 Å wavelength in the Stanford storage ring FEL is feasible according to this analysis. A small signal gain of 3.5, can be obtained at 320 Å wavelength in the third harmonic, using a wiggler of 8.3 cm period (case 2), whereas a wiggler of 6.4 cm period (case 3) produces a small signal gain of more than 5.5 at the fundamental ($\lambda = 285$ Å). It must be noted that this advantage of the fundamental over the higher harmonics is not obvious in general, especially not in the space-charge dominated regimes [15]. Also, the advantage of greater tunability of the longer period wiggler must be considered in selecting the final design.

References

[1] L.R. Elias, W. Fairbanks, J. Madey, H.A. Schwettman and T. Smith, Phys. Rev. Lett. 33 (1976) 413.
[2] D.A.G. Deacon, L.R. Elias, J.M.J. Madey, G.J. Ramain, H.A. Schwettman and T.I. Smith, Phys. Rev. Lett. 38 (1977) 892.
[3] M. Billardon, P. Elleaume, J.M. Ortega, C. Bazin, M. Bergher, M. Velghe, Y. Petroff, D.A.G. Deacon, K.E. Robinson and J.M.J. Madey, Phys. Rev. Lett. 51 (1983) 18, 1652.
[4] G.R. Neil, J.A. Edighoffer, S.W. Fornaca, C.E. Hess, T.I. Smith and H.A. Schwettman, Nucl. Instr. and Meth. A237 (1985) 199.
[5] J. Gea-Banacloche, G.T. Moore and M.O. Scully, Free Electron Generators of Extreme Ultraviolet Coherent Radiation, eds. J., M.J. Madey and C. Pellegrini, American Institute of Physics, Conf. Proc. Vol. 118 (1984) p. 161.
[6] J.B. Murphy and C. Pellegrini, Nucl. Instr. and Meth. A237 (1985) 159.
[7] J.M. Peterson, J.J. Bisognano, A.A. Garren, K. Halbach, K.J. Kim and R.C. Sah, Nucl. Instr. and meth. A237 (1985) 360.
[8] H. Weidemann, Proc. Int. Free Electron Laser Conf., Bendor, France (1982).
[9] J.C. Goldstein, B.E. Newnam, R.K. Cooper, J.C. Comly Jr, 2nd Topical meeting on Laser Techniques in the Extreme Ultraviolet, Boulder, CO (Mar 5–7, 1984).
[10] D.A.G. Deacon, these Proceedings (7th Int. FEL Conf.) Nucl. Instr. and Meth. A250 (1986) 262.
[11] D.T. Attwood, Free Electron Generators of Extreme Ultraviolet Coherent Radiation, eds., J.M.J. Madey and C. Pellegrini, American Institute of Physics, Conf. Proc. vol. 118 (1984) p. 294.
[12] A. Gover and P. Sprangle, IEEE J. Quantum Electron. QE-17 (1981) 1196.
[13] G. Dattoli, T. Letardi, J.M.J. Madey and A. Renieri, Nucl. Instr. and Meth. A237 (1985) 326.
[14] E. Jerby and A. Gover, IEEE J. Quantum Electron. (1985), QE-21 (1985) 1041.
[15] E. Jerby and A. Gover, these proceedings (7th Int. FEL Conf.) Nucl. Instr. and Meth. A250 (1986) 192.
[16] E. Jerby and A. Gover, to be published.
[17] G.T. Moore, Opt. Commun. 52 (1984) 46.
[18] E.T. Scharlemann, A.M. Sessler and J.S. Wurtele, Phys. Rev. Lett. 54 (1985) 1925.
[19] W.M. Fawley, D. Prosnitz and E.T. Scharlemann, Phys. Rev. A30 (1984) 2472.
[20] J.E. LaSala, D.A.G. Deacon and E.T. Scharlemann, these Proceedings (7th Int. FEL Conf.) Nucl. Instr. and Meth. A249 (1986).
[21] Ming Xie and D.A.G. Deacon, these Proceedings (7th Int. FEL Conf.) Nucl. Instr. and Meth. A249 (1986).